A New Adsorption Model Based on Generalized van der Waals Partition Function for the Description of All Types of Adsorption Isotherms

Lingli Kong and Hertanto Adidharma*

Department of Chemical Engineering, University of Wyoming, Laramie, Wyoming 82071-3295, USA

Abstract

A new adsorption model is proposed based on the Generalized van der Waals partition function by introducing the concept of attractive region, which integrates the effects of the adsorption sites of adsorbent and represents pore space where adsorbates concentrate. A theoretical expression for the chemical potential of adsorbates in the attractive region is derived and used to calculate the adsorbate density in each attractive region. The model can generate all the six types of isotherms classified by the International Union of Pure and Applied Chemistry (IUPAC) report including those with hysteresis and is easy to use. It is a generalized model that can be applied to various types of porous materials. With the fitted parameters, the model can predict the adsorption isotherms even for adsorbents with wide pore size distributions. It also well captures the isotherm-type transition as temperature changes and can estimate the hysteresis when capillary condensation exists.

Keywords

Isotherm types, hysteresis, Generalized van der Waals, square-well potential, adsorption

1 Introduction

Adsorption isotherms of porous materials are of great significance because they carry important equilibrium information that is required in many fields of industry, such as catalyst, gas storage, CO_2 capture, etc. Modeling of adsorption isotherms has been explored since more than a hundred years ago [1]. IUPAC report has classified the adsorption isotherms into six types [2], and the isotherm types mentioned

* Corresponding author. Tel: +1 307 766 2909.
E-mail address: adidharm@uwyo.edu

in this work are also based on this classification. Classical adsorption models such as Langmuir, Freundlich, Dubinin-Radushkevich (DR), Toth, Sips, etc. have been widely used because of their simplicity in forms and parameters. However, most of them are empirical models [3], none of them is able to generate the six types of isotherms listed in the IUPAC report, and researchers have to fit the parameters of a few models to decide which one best describes experimental data because the performance of the models is not consistent when the adsorbate/adsorbent pair is different [4]. Furthermore, the empirical parameters usually have little or no physical meanings.

The Brunauer-Emmett-Teller (BET) model can explain the formation of five types of isotherms, which is successfully applied to surface area prediction [5], but it is only applicable over a limited pressure range because of its assumptions [6,7]. Langmuir model, which was initially derived for adsorption on homogeneous surfaces, has been modified as multisite Langmuir model for heterogeneous surfaces. To take into account the interactions among adsorbates, the 'neighborhood' concept and more empirical parameters had to be introduced [8]. Still, the model is not applicable to all the isotherm types. Chakraborty, et al. [9] also modified the Langmuir adsorption isotherm equation and proposed a model that can generate isotherms of Types I, II, III, and V. The modification did overcome some limitations of some existing models, but the model could not generate isotherm of Type IV or VI. Recently, Ng, et al. [10] implemented an excellent approach by combining three concepts, i.e., the Homotattic Patch Approximation (HPA), the revised Langmuir model, and the fractional probability factor for the distribution of site energy sets, and proposed a universal isotherm model for predicting different types of adsorption isotherms. However, the approach is inherently unable to describe isotherm with hysteresis.

To develop adsorption isotherm models, approaches based on kinetic consideration [11], thermodynamics [12], and potential theory [13] have all been employed, but there is always a gap between simplicity and accuracy in the adsorption isotherm modeling work. The modeling of molecular adsorption with a solid theoretical ground has been performed using statistical mechanics [14], where simplified expressions for five of the adsorption isotherm types were derived based on the grand

canonical partition function, but different types of isotherms were described by different forms of the grand canonical partition function. Such an approach leads to complicated analyses and many simplifications have to be made so that the modeling work can be performed. Due to the complexity of molecular interactions (among molecules and between adsorbate and adsorbent), and the adsorbent materials (porosity, the pore shapes, and pore size distribution, etc.), various phenomena can happen in the physisorption process, such as monomolecular/ multimolecular adsorption, monolayer/multilayer adsorption, condensation, etc. [14] There is not a model that can describe all the physisorption phenomena, including capillary condensation and hysteresis, and the model will either be simple but unable to describe all types and features of isotherms or accurate but complicated [15].

In this work, based on the Generalized van der Waals canonical partition function, we propose an engineering model, which, for the first time, is able not only to describe the six types of isotherms, but also to estimate the hysteresis when capillary condensation exists. We note that most classical models either use some factors/coefficients to account for the heterogeneity of the adsorbents, such as the structural heterogeneity factor in Chakraborty's modified Langmuir model [9], which cannot describe all of the adsorption phenomena caused by the heterogeneity of the adsorbents, or increase the types of adsorption sites, which will significantly increase the number of parameters. We balance this problem by introducing the concept of *attractive regions*, which are a coarse representation of adsorption sites. Attractive regions integrate the effects of adsorption sites and are flexible in reflecting the heterogeneity of the adsorbent. In other words, the model is not built on the basis of the surface, but the effects of the attractive sites. Because of the flexibility of the attractive regions, our model can deal with both multilayer and pore-filling adsorption and can be applied to a wide range of adsorbents, from adsorbents with nanopores to those with macropores, and from the crystal materials with homogeneous pore size to materials with wide pore size distribution (PSD) like activated carbons. Besides the simplicity in forms, the parameters of the model all have physical meanings.

2 Model

Porous materials can be of different types with various structures, which makes the distribution of adsorption sites not well-defined. For porous materials with crystal structures (e.g. MOFs, zeolites), it will be incomplete to assume that the adsorption phenomena depend only on the surfaces of the pore walls because as pressure increases, multiple adsorption sites could appear in the space of the pore rather than just on the surface of the adsorbents [16]. To avoid dealing with the complicated situations caused by the diversity of porous materials, we choose to focus on the overall effect of the adsorption sites. Since the confined fluid can accumulate in a layering pattern [17] or appear as clusters inside the pores [18], to create a model that is applicable to different cases, we treat the spaces where adsorbates concentrate, no matter in the form of films or clusters, as attractive regions with certain attractive potentials representing the adsorbent-adsorbate interactions. Figure 1 presents two examples of the distribution of a confined fluid in pore space. Figure 1 (a) shows the distribution in a pore with a homogeneous pore surface where the adsorbate molecules appear as a film in the regions close to the surface of the pore wall. Figure 1 (b) shows the distribution in a pore with a heterogeneous pore surface where adsorbates cluster to different places. Regions with the same attractive potential are considered to be of the same type containing adsorbates of the same average densities. They can appear at multiple places in the same pore as shown in Figure 1(b), where the labeled numbers in different attractive regions represent the region types. Besides the attractive regions, there can be spaces that are not affected by the adsorbent, referred to as non-attractive regions in Figure 1, the density in which is approximated by that of the bulk phase in our model. By calculating the average density in each type of attractive region, our model can obtain the total adsorbed amount if the total volume of each type of region is known. Therefore, we do not need to investigate the number or the shapes of spaces that have the same attractive potential and only the total volume of them is needed.

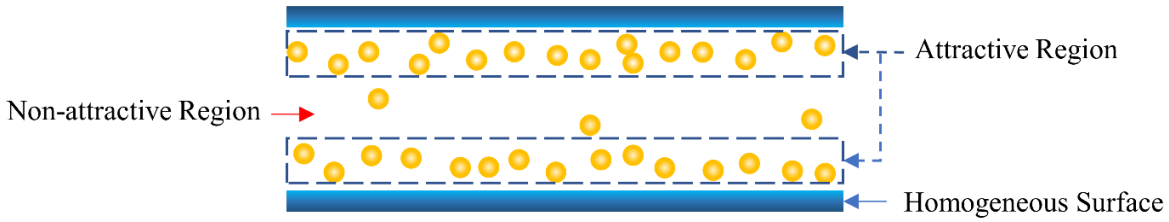

(a) Pore with homogeneous wall

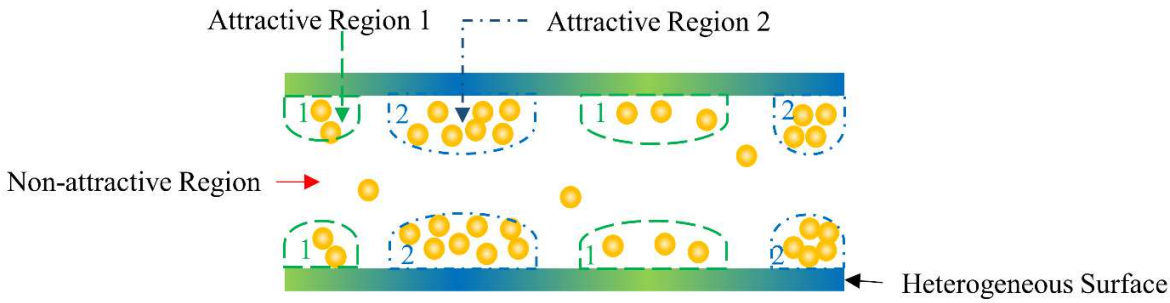

(b) Pore with heterogeneous wall

Figure 1. Attractive regions in pores of different surface properties with different adsorbate distributions

Since the whole system is in equilibrium and the fluids in different types of attractive regions have different densities, we regard these fluids as being at different states or adsorbed phases because they are under the influence of different attractive potentials. These different adsorbed phases could explain multiple sharp increases on isotherms. The separation of the confined fluid into different 'phases' may also help to explain the phenomenon that the confined fluid of some materials can have multiple condensation points or critical points [19]. Classical models are having difficulties in generating adsorption isotherms of Types II, IV, and VI, where a second sharp increase appears as pressure increases. In our model, we can simply solve this problem by assigning different types of attractive regions. Each sharp increase on the isotherm represents a filling process of adsorbates in one type of the attractive regions. In other words, the number of sharp increases on an adsorption isotherm is the basis of determining the number of types of the attractive regions. There are two types of sharp increase on

isotherm, i.e., (1) a section that has a steep slope and (2) a section close to the saturation pressure of the adsorbate that has increasing slopes (concave upward).

In some cases, the adsorbates inside a pore can form clusters of different densities in several places, but the overall isotherm does not show the corresponding number of sharp increases on isotherm. Since we determine the number of types of attractive regions based on the number of sharp increases on isotherm, each type of attractive region in the model might contain several clustered adsorbates with different densities, which means that the density calculated for each type of attractive regions for such cases is, in fact, the average density of these clustered adsorbates.

To predict the adsorbate density in one attractive region, we simply equalize the chemical potential of the adsorbate in that region to that in the bulk phase μ_b, which is:

$$\mu_b = kT[\ln(\Lambda^3)] + kT[\ln(\rho_{ig})] + kT\ln(\varphi) \quad (1)$$

where ρ_{ig} (= P/kT) is the number density of the ideal gas, Λ is the de Broglie wavelength of the molecules, P is the pressure, T is the temperature, k is the Boltzmann constant, and φ is the fugacity coefficient of the bulk phase.

The calculation of the chemical potential in the attractive region is based on the Generalized van der Waals canonical partition function $Q(T, V, N)$:

$$Q(T,V,N) = \left(\frac{q_{int}^N}{\Lambda^{3N}N!}\right) V_f^N \exp\left(\int_\infty^T \frac{E_{conf}}{kT^2}\,dT\right) \quad (2)$$

where, V is the region volume, N is the number of molecules in the region, q_{int} is the internal energy partition function for one molecule, V_f is the free volume of the hard-core fluid, and E_{conf} is the configurational energy. The expression of the chemical potential μ is:

$$\mu = -kT\left[\frac{\partial\ln(Q)}{\partial N}\right]_{T,V} \quad (3)$$

To simplify the model, we use square-well potential to represent the interactions among adsorbates and between adsorbates and adsorbents. We assume that in each attractive region, a constant attractive potential $-\varepsilon_p$ is homogeneously distributed. Thus, the expression of the configuration energy in the attractive region is:

$$E_{conf} = -\frac{N}{2} N_c \varepsilon - N\varepsilon_p \tag{4}$$

where the first term represents the energy generated by the interactions among the adsorbates in the attractive region, the second term represents the energy from adsorbate-adsorbent interactions in the attractive region, and $-\varepsilon$ is the well potential of the adsorbate-adsorbate interactions. The expression of the configuration number N_c is:

$$N_c = 4\pi\rho \int g(r,\rho,T) r^2 dr \tag{5}$$

where ρ is the number density in the attractive region, and we use the low-density radial distribution function for square-well fluid to approximate $g(r, \rho, T)$:

$$g(r) = \begin{cases} 0 & r < \sigma \\ exp\left(\frac{\varepsilon}{kT}\right) & \sigma \le r \le \lambda\sigma \\ 1 & r > \lambda\sigma \end{cases} \tag{6}$$

where r is the center to center distance between two molecules, σ is the molecule diameter, and $\lambda\sigma$ is the range of the potential well. The parameters for adsorbates (ε, σ, λ) in this work are obtained from SAFT2 equation of state and can be found in our previous work [20]. Therefore, we can rewrite the expression of the configuration number as:

$$N_c = Cexp\left(\frac{\varepsilon}{kT}\right)\rho^* \tag{7}$$

where ρ^* ($= \rho\sigma^3$) is the reduced density in the attractive region, and C is the reduced volume for the potential well of a molecule within the attractive region, which is, in fact, a function of the geometrical shape and size of the attractive region [20,21]. Since our model in this work is a generalized model for all

types of porous materials, we do not have a generalized expression for C, but we do know its magnitude range, i.e., [0, $4\pi(\lambda^3\text{-}1)/3$]. When an attractive region is so tiny that it can only hold one molecule inside, the reduced volume is set to 0. The upper limit of the reduced volume is the same as that of bulk phase, which means that the attractive region is so large that the molecule in the attractive region can be considered the same as that in bulk fluid, i.e., $4\pi(\lambda^3\text{-}1)/3$.

The other important parameter in Eq. (2) is the free volume V_f, which is expressed as:

$$V_f = V - \frac{N}{\rho_{max}} \tag{8}$$

where V is the volume of the attractive region and ρ_{max} is the close-packed density. As we have mentioned in our previous work [20], there exists an inaccessible region between the attractive region and the adsorbent, and we can use the reduced close-packed density in the bulk phase ($\sqrt{2}$) to represent that in the attractive regions. However, for molecular sieves whose pore sizes are as small as 4Å or 5Å, the influence of the pore walls is significant, and this approximation could be less accurate.

Since the model does not distinguish the shapes or sizes of attractive regions that have the same attractive potential, the expression of the chemical potential for attractive regions of type i is then:

$$\mu_i = kT\left\{[\ln(\Lambda^3)] - \left[\ln\left(\frac{1}{\rho_i} - \frac{1}{\rho_{max}}\right)\right] + \frac{\rho_i}{\rho_{max}-\rho_i} - C_i\rho_i\left[\exp\left(\frac{\varepsilon}{kT}\right) - 1\right] - \frac{\varepsilon_{p,i}}{kT}\right\} \tag{9}$$

where we use subscript i to represent the parameters or variables in attractive regions of type i. By equalizing the chemical potential of the adsorbate in a certain type of attractive region to that of the bulk phase, i.e.,

$$\mu_i = \mu_b \tag{10}$$

we can calculate the number density of adsorbate in that attractive region.

As our model can be written in the form of van der Waals equation, a sigmoid van der Walls loop of isotherm can exist when there is capillary phase transition (capillary condensation) and therefore, one,

two, or three real positive roots can be obtained depending on the parameters of the attractive region, pressure, and temperature. If we find more than one real positive root, hysteresis should occur at that particular condition. The physical meaning of the roots and the sigmoid van der Waals loop obtained by our model are described in detail in the Supplementary Material.

To write the equation above in terms of per mole, the chemical potential is expressed as:

$$\mu_{molar,i} = RT\left[ln\left(\frac{\Lambda^3 N_{av}}{v_i - b}\right) + \frac{b}{v_i - b}\right] - \frac{2a_i}{v_i} - N_{av}\varepsilon_{p,i} \tag{11}$$

$$a_i = N_{av}^2 \frac{C_i \sigma^3}{2} kT\left[exp\left(\frac{\varepsilon}{kT}\right) - 1\right] \tag{12}$$

$$b = \frac{N_{av}}{\rho_{max}} \tag{13}$$

where v_i is the molar volume, a_i and b are the van der Waals parameters. Eq. (11) is the van der Waals expression for the chemical potential in attractive regions.

The density and the fugacity coefficient of the bulk phase are both calculated by SAFT2 equation of state [22]. The predicted absolute adsorbed amount is then given by:

$$Ads = [\sum_i^n f_i \rho_i + (1 - \sum_i^n f_i)\rho_{bulk}]V_{total} \tag{14}$$

where n is the number of attractive regions, V_{total} is the total pore volume, f_i is the fraction of the total pore volume that one type of attractive region occupies, ρ_i can be obtained from Eq. (10), which is a simple implicit equation with ρ_i as the only unknown, and ρ_{bulk} is the bulk phase density. The excess adsorbed amount Ads^{ex}, which is commonly used, can be expressed as follows:

$$Ads^{ex} = Ads - \rho_{bulk}V_{total} = [\sum_i^n f_i(\rho_i - \rho_{bulk})]V_{total} \tag{15}$$

Sometimes isotherm is presented in a reduced form [2], which is a plot of α_s versus the relative pressure P/P_0, where P_0 is the saturation pressure of the adsorbate and α_s is expressed as:

$$\alpha_s = \frac{Ads^{ex}}{Ads_{ref}^{ex}} \quad \text{or} \quad \alpha_s = \frac{Ads}{Ads_{ref}} \tag{16}$$

In Eq. (16), the denominator is the normalizing factor, which is the value of Ads^{ex} or Ads at a preselected relative pressure (P/P_0 = 0.4 is generally used). Note that it is possible to fit the model parameters to the reduced form of the isotherm and use Eq. (15) to roughly estimate the total pore volume of adsorbent. For the figures in this work, isotherms in terms of adsorbed amount are presented using absolute adsorbed amount and isotherms in terms of reduced adsorbed amount are obtained based on excess adsorbed amount.

To test the ability of the model in generating different types of isotherms and track the change of the adsorbed amount as pressure increases, we simply assign 20% of the total pore volume for the regions not influenced by the adsorbent and vary the parameters of the attractive regions, which occupy 80% of the total pore volume. These fractions are arbitrarily chosen just to provide an example and generate fictitious isotherms. Figure 2 presents the N_2 adsorption isotherms in terms of the reduced densities at 77 K in fictitious adsorbents, and the parameters of the attractive regions are listed in Table 1. By assigning one type of attractive region in the pore space and varying the parameters, we can obtain isotherms of Types I, III, and V, as shown in Figure 2 (a). Note that for Type I and V isotherms, each has one sharp increase, i.e., a section that has a very steep slope, and for Type III, it has one sharp increase, i.e., a section close to the saturation pressure that has increasing slopes (concave upward), although the isotherm must stop at P/P_0 = 1. By comparing the parameters for isotherms of Types III and V without hysteresis, we can see that Type III isotherm is generated when the interaction between adsorbate and adsorbent is relatively weak. Figure 2 (b) presents the isotherms of Types II, IV, and VI. For isotherms of Types II and IV, we assign two types of attractive regions to feature the two sharp increases on the isotherms. We give an example of isotherm Type VI with three steps in Figure 2 (b).

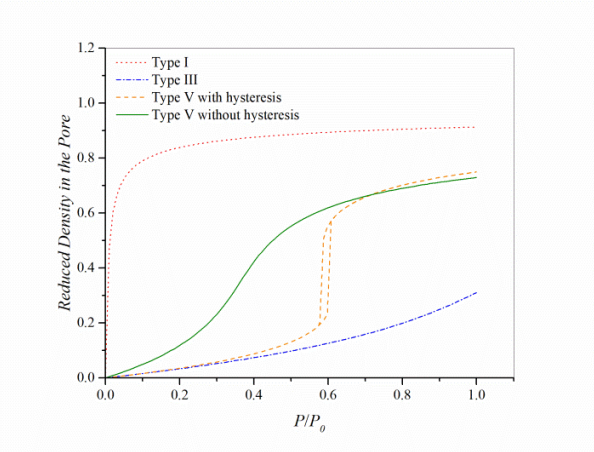

(a) Isotherms with one type of attractive regions in the pore

(b) Isotherms with two or more types of attractive regions in the pore

Figure 2. Isotherm types generated by the model

Table 1. Parameters (f_i, $\varepsilon_{p,i}/k$(K), C_i) of different types of attractive regions for isotherms in Figure 2

Type I	(0.8, 800, 0.5)
Type III	(0.8, 320, 1.5)
Type V (with hysteresis)	(0.8, 320, 2.0)
Type V (without hysteresis)	(0.8, 400, 1.5)
Type II	(0.12, 800, 0.5), (0.68, 320, 1.5)
Type IV (with hysteresis)	(0.16, 800, 0.5), (0.64, 320, 2.0)
Type IV (without hysteresis)	(0.40, 800, 0.5), (0.40, 400, 1.5)
Type VI	(0.32, 800, 0.5), (0.32, 400, 1.5), (0.16, 480, 1.5)

3 Results and discussion

Our model is applied to predict different types of isotherms and compared with experimental data. In Figures 3 to 7, lines are the isotherms generated by models and points are experimental data from

literature. For the isotherms presented in this section, only one of the isotherms (or two of the isotherms for adsorbent with a wide PSD) is fitted and the rest are predicted using the parameters obtained from fitting.

3.1 Prediction of different types of isotherms

Figure 3 presents the performance of the model in predicting Type I isotherm, where one type of attractive region is assigned to our model. In Figure 3 (a), multisite Langmuir model, which is based on multilayer mechanism, DR model, which is based on pore-filling mechanism, and our model are fitted to the isotherm of CH_4 in Zeolite 13X [23] at 298 K. All of the models can perfectly fit the data with coefficient of determination of 0.9995 for our model, 0.9996 for multisite Langmuir model, and 0.9996 for DR model. Therefore, the lines for these three models at 298 K in Figure 3 (a) coincide. By using the fitted parameters of the models, isotherm at 323 K is predicted. Noticeably, the isotherm predicted by our model, with an average absolute deviation (ARD) of 6.8 %, can better capture the curvature of the experimental isotherm and the effect of temperature. The performance of multisite Langmuir and DR models is far from satisfactory with ARDs of 41.8 % and 16.8 %, respectively. To obtain reasonable parameters for these two models, all of the isotherms should be fitted together as mentioned in reference [23]. The expressions and the fitted parameters for Langmuir, DR, and models that will appear later for comparisons, i.e., BET and the universal model [10], can be found in the Supplementary Material.

According to our previous work [20], there is more than one type of attractive regions in IRMOF-1. Since we only assign one attractive region, the predicted isotherms slightly disagree with the experimental data [24], as seen in Figure 3 (b), but the model in this work is much simpler than that in our previous work and the overall performance is still reasonable. The temperature dependence of the predicted isotherms could also be improved by considering the temperature dependence of the square-well potential parameters, which is commonly considered to improve the performance of such a simple interaction potential model. We will explore this extension in our future work.

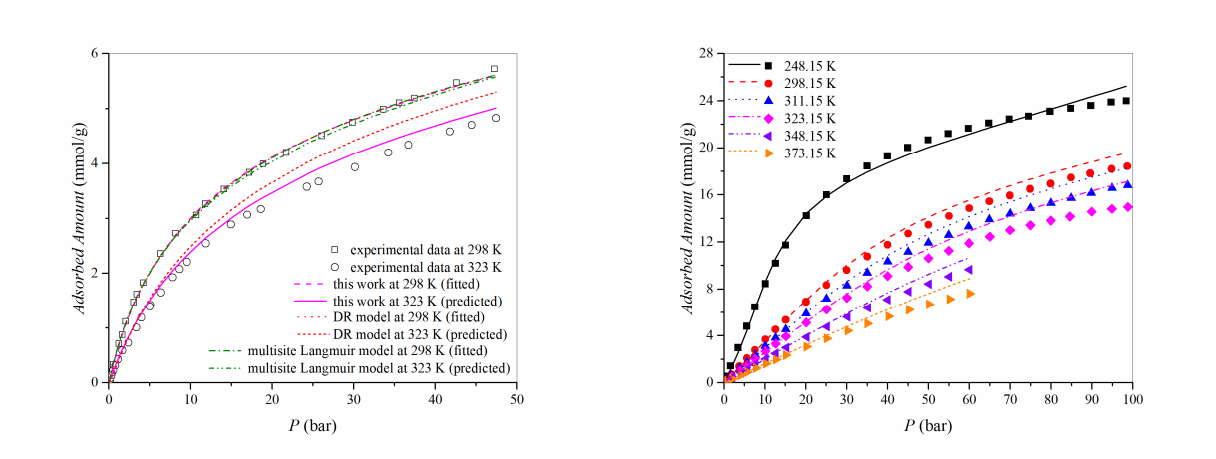

(a) CH_4 adsorption in Zeolite 13X (data fitted at 298 K)

(b) CH_4 adsorption in IRMOF-1 (data fitted at 248.15 K)

Figure 3. Isotherm prediction of Type I in crystal adsorbents; experimental data [23,24] (points) and calculated (lines)

Figure 4 is the adsorption isotherm of N_2 in terms of reduced adsorbed amount in macroporous material carbon black Cabot BP 280 [25]. With two types of attractive region assigned, the correlated Type II isotherm is in good agreement with the experimental data. BET model is also fitted to the experimental data for comparison. As shown in Figure 4, the BET model fails at higher pressure.

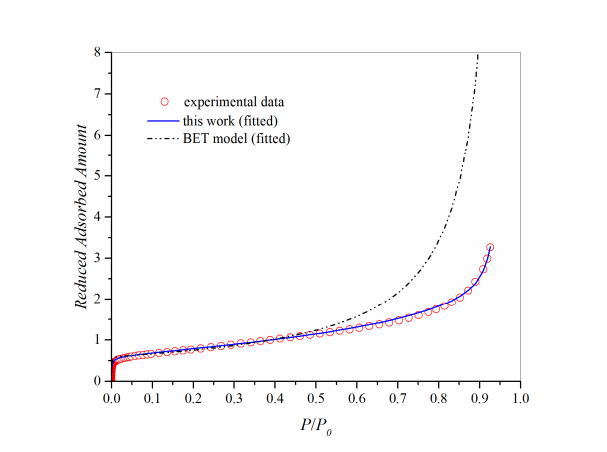

Figure 4. N_2 adsorption in Cabot BP 280 at 77 K; experimental data [25] (points) and calculated (lines)

Figure 5 presents the adsorption isotherms for CO_2 in IRMOF-1 [26]. One type of attractive region is assigned to our model, and the parameters are fitted to the isotherm at 218 K. The model captures the shift of isotherm type from Type V to Type III as temperature increases. To predict the condensation point on an isotherm, researchers tend to specially build models for it [27] and it is not easy to find an adsorption model that can both predict the adsorption isotherm and the condensation point. Even the Grand Canonical Monte Carlo Simulation cannot predict these two adsorption features with high accuracies at the same time [26]. As shown in Figure 5, the predictions of the hysteresis loops of our model on the isotherms are reasonable. Since we use constant values of parameters for all different temperatures in our model, noticeable errors can be found in the predicted isotherms at 208 K and 195 K. The interaction potentials among adsorbates and between adsorbate and adsorbent can in fact increase as temperature decreases. To obtain more accurate prediction of the temperature effect, the potential parameters (ε, ε_p) could be made as functions of temperature, which would be explored in our future work.

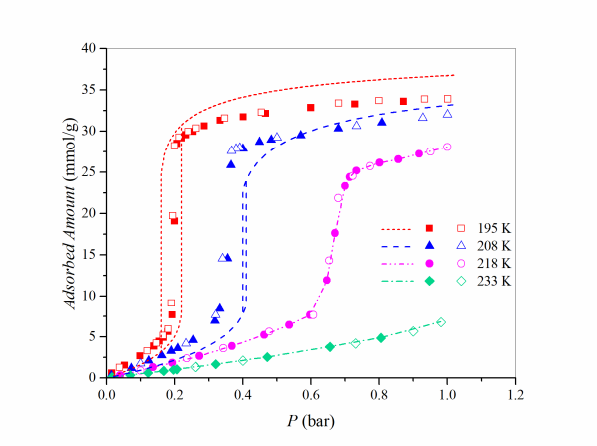

Figure 5. CO_2 adsorption in IRMOF-1; adsorption data [26] (filled points), desorption data [26] (open points), and calculated (lines).

The prediction of Type IV isotherm using a simple engineering model is usually unsatisfactory [28] but our model can predict the isotherms of Type IV accurately. Figure 6 is the N_2 adsorption in MCM-41 [29] where our model and the universal model proposed by Ng, et. al. [10], which is the only engineering model we find that can also generate all the six types of isotherms, are compared. With

parameters fitted at 67.8 K, both models are used to predict isotherms at 63.3 K. Unfortunately, the predictability of the universal model is far from satisfactory. More specifically, the universal model cannot be used to predict isotherms at different temperatures unless the parameters are fitted to all of these isotherms. Whereas, our model can predict the isotherms at lower temperatures and capture the hysteresis correctly. In Figures 5 and 6, although the predictions of hysteresis show noticeable errors compared to the experimental data, our model is the first model that can provide such estimations for real systems.

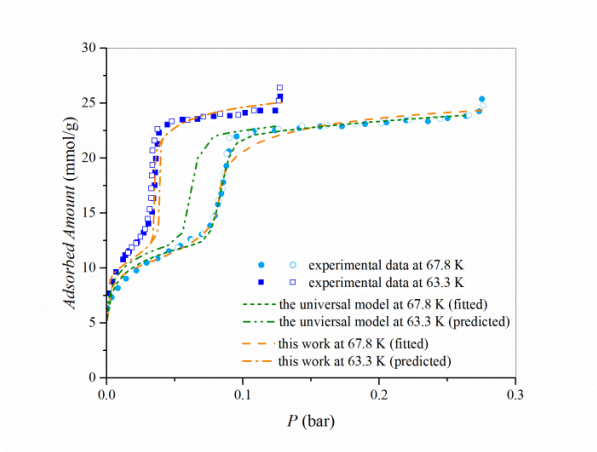

Figure 6. N_2 adsorption in MCM-41; adsorption data [29] (filled points), desorption data [29] (open points), and calculated (lines).

Figure 7 shows the isotherm of CH_4 adsorption in MgO [30] at 87.4 K, which is Type VI isotherm. Four types of attractive regions are assigned to our model since four sharp increases are observed on the isotherm. The calculated isotherm can represent the experimental data, which indicates that our model can well capture the features of Type VI isotherm.

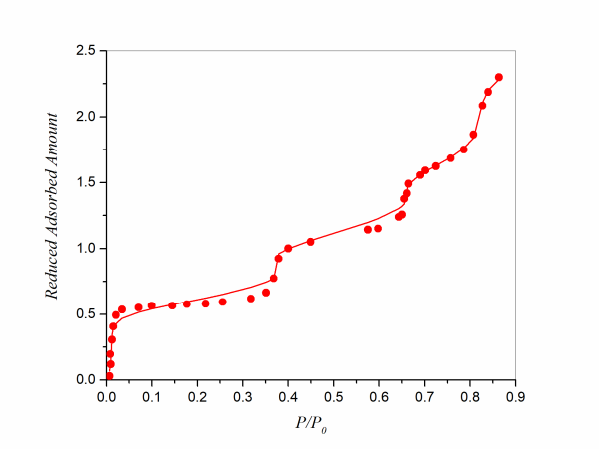

Figure 7. CH_4 adsorption in MgO at 87.4 K; experimental data [30] (points) and calculated (line).

3.2 Predictions for adsorbent with a wide PSD

For porous materials with wide PSD or pores of different sizes distributed irregularly, e.g., activated carbons, the attractive force generated by the atoms of adsorbent can overlap in different patterns in pores of different sizes, unless the material has macropores where the overlap barely happen [21]. As a result, the distributions of attractive force and adsorbates in different pores can be very different and it would be less possible to find regions of the same attractive potential or the same average adsorbate density. Thus, the presumed number of types of attractive regions is not able to capture all the features of the adsorption isotherms and it is not safe to use parameters fitted to one isotherm to predict isotherms at other temperatures. By increasing the number of types of attractive regions, more features can be captured, but the model will become more complicated and have more parameters. Therefore, instead of increasing the number of attractive regions, we choose to use parameters that are fitted to two isotherms to predict the isotherms at other temperatures so that we can average the effect of the pore size distribution on the attractive regions.

The adsorption isotherms for CH_4 in Honeycomb Monolith activated carbon [31] are presented in Figure 8. One type of attractive region is assigned to the adsorbent because the isotherm is of Type I, and the parameters are fitted to isotherms at 299 K and 423 K because the material has a wide PSD and pores

of different sizes are irregularly distributed. The coefficient of determination for fitting of isotherms at 299 K and 423 K are 0.9855 and 0.9003, respectively, and the ARDs for the predicted isotherms at 323 K, 348 K, and 373 K are 8.8 %, 9.1 %, and 10.6 %, respectively. Although the model with one type of attractive region cannot completely represent the various adsorption phenomena in different pores, the predicted isotherms have the right curvature and capture the effect of temperature. The relatively larger errors of the predicted isotherms in Figure 8, especially at high pressures, shows that the influence of a wide PSD can be important.

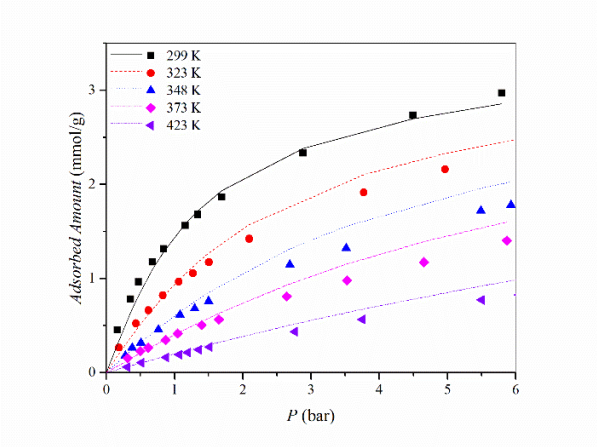

Figure 8. Isotherm prediction of Type I in activated carbons; experimental data [31] (points) and calculated (lines)

Table 2 lists the parameters of our model obtained using the least-square method that are used to produce the isotherms in Figures 3 to 8.

Table 2. The model parameters of different adsorbents

Adsorbent	V_{total} (cm^3/g)	Adsorbate	(f_i, ε_{pi}/k (K), C_i)
Zeolite 13X	0.478 [23]	N_2	(0.23, 1230, 0.0)
		CH_4	(0.31, 1387, 0.0)
IRMOF-1	1.315 [26]	CH_4	(0.32, 852, 3.6)
		CO_2	(0.48, 1135, 1.4)

Honeycomb Monolith	0.334 [31]	CH_4	(0.21, 1943, 2.2)
MCM-41	0.871 [29]	N_2	(0.20, 944, 0.0), (0.30, 416, 1.5)
Cabot BP 280		N_2	(0.65, 298, 1.9), (0.07, 1052, 0.0)
MgO		CH_4	(0.12, 965, 1.3), (0.09, 628, 1.5), (0.10, 572, 1.4), (0.29, 587, 1.4)

4 Conclusions

For the adsorption of light gases, we propose a model based on the Generalized van der Waals partition function that can generate all the six types of adsorption isotherms classified by IUPAC report, including those with hysteresis, and predict the adsorbed amount in various types of porous materials. We overcome the difficulty in describing the pore shape and pore size by introducing the concept of attractive region, which is the region where adsorbates accumulate inside the pore. Since the attractive region reflects the overall attractive force from some parts of the adsorbent, the heterogeneity of the surface will not influence the form of the model. The number of types of attractive regions is considered to be equal to the number of sharp increases on the adsorption isotherm.

The model has been applied to describe the adsorptions of real gases in different types of adsorbents that have isotherms of Types I through VI. In general, parameters fitted to one isotherm can be used to predict isotherms at other temperatures. In the case of porous materials with wide PSD or pores of different sizes distributed irregularly, two isotherms are used to fit the parameters so that the effect of the pore size distribution on the attractive regions can be averaged and isotherms at other temperatures can be more accurately predicted. It is also found that the model can well capture the isotherm-type transition as temperature changes and estimate the hysteresis when capillary condensation exists.

The model developed is therefore a generalized model that can be applied to a wide range of adsorbents, from adsorbents with nanopores to those with macropores, and from the crystal materials with homogeneous pore size to materials with wide pore size distribution (PSD).

Acknowledgement

This work was supported by the State of Wyoming and the Department of Energy (DE-PI0000017).

References

[1] A. Dabrowski, Adsorption-from theory to practice, Adv. Colloid Interface Sci. 93 (2001) 135–224. doi:10.1016/S0001-8686(00)00082-8.

[2] M. Thommes, K. Kaneko, A. V. Neimark, J.P. Olivier, F. Rodriguez-Reinoso, J. Rouquerol, K.S.W. Sing, Physisorption of gases, with special reference to the evaluation of surface area and pore size distribution (IUPAC Technical Report), Pure Appl. Chem. 87 (2015) 1051–1069. doi:10.1515/pac-2014-1117.

[3] B.H. Foo, K.Y., Hameed, Insights into the modeling of adsorption isotherm systems, Chem. Eng. 156 (2010) 2–10. doi:10.1016/j.cej.2009.09.013.

[4] A. Ladshaw, S. Yiacoumi, C. Tsouris, D. DePaoli, Generalized gas-solid adsorption modeling: Single-component equilibria, Fluid Phase Equilib. 388 (2015) 169–181. doi:10.1016/j.fluid.2015.01.003.

[5] S. Brunauer, P.H. Emmett, The use of low temperature van der Waals adsorption isotherms in determining the surface areas of various adsorbents, J. Am. Chem. Soc. 59 (1937) 2682–2689. doi:10.1021/ja01291a060.

[6] Y. Tian, J. Wu, A comprehensive analysis of the BET area for nanoporous materials, AIChE J. 64 (2018) 286–293. doi:10.1002/aic.15880.

[7] D. Dollimore, P. Spooner, A. Turner, The bet method of analysis of gas adsorption data and its relevance to the calculation of surface areas, Surf. Technol. 4 (1976) 121–160. doi:10.1016/0376-4583(76)90024-8.

[8] J.U. Keller, J.D. Popernack, R. Staudt, A Generalization of Langmuirs adsorption isotherm to admolecules with interaction, Adsorpt. Sci. Technol. (2000) 336–340. doi:10.1142/9789812793331_0067.

[9] A. Chakraborty, B. Sun, An adsorption isotherm equation for multi-types adsorption with thermodynamic correctness, Appl. Therm. Eng. 72 (2014) 190–199. doi:10.1016/j.applthermaleng.2014.04.024.

[10] K.C. Ng, M. Burhan, M.W. Shahzad, A. Bin Ismail, A universal isotherm model to capture adsorption uptake and energy distribution of porous heterogeneous surface, Sci. Rep. 7 (2017) 1–11. doi:10.1038/s41598-017-11156-6.

[11] H. Qiu, L. Lv, B. Pan, Q. Zhang, W. Zhang, Q. Zhang, Critical review in adsorption kinetic models, J. Zhejiang Univ. A. 10 (2009) 716–724. doi:10.1631/jzus.A0820524.

[12] J.W. Gibbs, On the equilibrium of heterogeneous substances, Am. J. Sci. 16 (1878) 441–458. doi:10.2475/ajs.s3-16.96.441.

[13] M.M. Dubinin, The potential theory of adsorption of gases and vapors for adsorbents with energetically nonuniform surfaces., Chem. Rev. 60 (1960) 235–241. doi:10.1021/cr60204a006.

[14] M. Khalfaoui, S. Knani, M.A. Hachicha, A. Ben Lamine, New theoretical expressions for the five adsorption type isotherms classified by BET based on statistical physics treatment, J. Colloid Interface Sci. 263 (2003) 350–356. doi:10.1016/S0021-9797(03)00139-5.

[15] J. U. Keller, R. Staudt, Gas adsorption equilibria: experimental methods and adsorptive isotherms, Springer, New York, 2011.

[16] D. Dubbeldam, H. Frost, K.S. Walton, R.Q. Snurr, Molecular simulation of adsorption sites of light gases in the metal-organic framework IRMOF-1, Fluid Phase Equilib. 261 (2007) 152–161. doi:10.1016/j.fluid.2007.07.042.

[17] D.L. Goodstein, J.J. Hamilton, Thermodynamic study of methane multilayers adsorbed on graphite, Phys. Rev. B. 28 (1983) 3838–2848.

[18] N.S. Suraweera, R. Xiong, J.P. Luna, D.M. Nicholson, D.J. Keffer, On the relationship between the structure of metal-organic frameworks and the adsorption and diffusion of hydrogen, Mol. Simul. 37 (2011) 621–639. doi:10.1080/08927022.2011.561432.

[19] N. Höft, J. Horbach, Condensation of methane in the metal–organic framework IRMOF-1: evidence for two critical points, J. Am. Chem. Soc. 137 (2015) 10199–10204. doi:10.1021/jacs.5b04077.

[20] L. Kong, H. Adidharma, A generalized van der Waals model for light gas adsorption prediction in IRMOFs, Phys. Chem. Chem. Phys. 21 (2019) 8906–8914. doi:10.1039/c9cp00285e.

[21] L. Kong, H. Adidharma, Adsorption of simple square-well fluids in slit nanopores: modeling based on generalized van der Waals partition function and Monte Carlo simulation, Chem. Eng. Sci. 177 (2018) 323–332. doi:10.1016/j.ces.2017.11.025.

[22] S.P. Tan, X. Ji, H. Adidharma, M. Radosz, Statistical associating fluid theory coupled with restrictive primitive model extended to bivalent ions. SAFT2: 1. Single salt + water solutions, J. Phys. Chem. B. 110 (2006) 16694–16699. doi:10.1021/jp0625107.

[23] S. Cavenati, C.A. Grande, A.E. Rodrigues, Adsorption equilibrium of methane, carbon dioxide, and nitrogen on zeolite 13X at high pressures, J. Chem. Eng. Data. 49 (2004) 1095–1101. doi:10.1021/je0498917.

[24] J.A. Mason, M. Veenstra, J.R. Long, Evaluating metal-organic frameworks for natural gas storage, Chem. Sci. 5 (2014) 32–51. doi:10.1039/c3sc52633j.

[25] M. Kruk, M. Jaroniec, K.P. Gadkaree, Nitrogen adsorption studies of novel synthetic active carbons, J. Colloid Interface Sci. 192 (1997) 250–256. doi:10.1006/jcis.1997.5009.

[26] K.S. Walton, A.R. Millward, D. Dubbeldam, H. Frost, J.J. Low, O.M. Yaghi, R.Q. Snurr, Understanding inflections and steps in carbon dioxide adsorption isotherms in metal-organic frameworks, J. Am. Chem. Soc. 130 (2008) 406–407. doi:10.1021/ja076595g.

[27] S.Z. Qiao, S.K. Bhatia, X.S. Zhao, Prediction of multilayer adsorption and capillary condensation phenomena in cylindrical mesopores, Microporous Mesoporous Mater. 65 (2003) 287–298. doi:10.1016/j.micromeso.2003.08.018.

[28] L. Travalloni, M. Castier, F.W. Tavares, S.I. Sandler, Thermodynamic modeling of confined fluids using an extension of the generalized van der Waals theory, Chem. Eng. Sci. 65 (2010) 3088–3099. doi:10.1016/j.ces.2010.01.032.

[29] K. Morishige, H. Fujii, M. Uga, D. Kinukawa, Capillary critical point of argon, nitrogen, oxygen, ethylene, and carbon dioxide in MCM-41, Langmuir. 13 (1997) 3494–3498. doi:10.1021/la970079u.

[30] J.M. Gay, J. Suzanne, J.P. Coulomb, Wetting, surface melting, and freezing of thin films of methane adsorbed on MgO(100), Phys. Rev. B. 41 (1990) 11346–11351. doi:10.1103/PhysRevB.41.11346.

[31] D. Saha, K. Nelson, J. Chen, Y. Lu, S. Ozcan, Adsorption of CO_2, CH_4, and N_2 in micro-mesoporous nanographene: a comparative Study , J. Chem. Eng. Data. 60 (2015) 2636–2645. doi:10.1021/acs.jced.5b00291.